Proceedings of the Combustion Institute, Volume 28, 2000/pp. 1563–1577

INVITED TOPICAL REVIEW

CHEMICAL KINETICS OF HYDROCARBON IGNITION IN PRACTICAL COMBUSTION SYSTEMS

CHARLES K. WESTBROOK
Lawrence Livermore National Laboratory
Livermore, CA 94550, USA

Chemical kinetic factors of hydrocarbon oxidation are examined in a variety of ignition problems. Ignition is related to the presence of a dominant chain-branching reaction mechanism that can drive a chemical system to completion in a very short period of time. Ignition in laboratory environments is studied for problems including shock tubes and rapid compression machines. Modeling of the laboratory systems is used to develop kinetic models that can be used to analyze ignition in practical systems. Two major chain-branching regimes are identified, one consisting of high temperature ignition with a chain branching reaction mechanism based on the reaction between atomic hydrogen with molecular oxygen, and the second based on an intermediate temperature thermal decomposition of hydrogen peroxide. Kinetic models are then used to describe ignition in practical combustion environments, including detonations and pulse combustors for high temperature ignition and engine knock and diesel ignition for intermediate temperature ignition. The final example of ignition in a practical environment is homogeneous charge, compression ignition (HCCI), which is shown to be a problem dominated by the kinetics of intermediate temperature hydrocarbon ignition. Model results show why high hydrocarbon and CO emissions are inevitable in HCCI combustion. The conclusion of this study is that the kinetics of hydrocarbon ignition are actually quite simple, since only one or two elementary reactions are dominant. However, many combustion factors can influence these two major reactions, and these are the features that vary from one practical system to another.

Introduction

In many practical steady combustion systems, ignition is simply a means of starting the system on its way to steady state. Performance and emissions are essentially independent of ignition in such systems as boilers, furnaces, and burners. However, in other practical problems, ignition has a great influence on performance, emissions, and other characteristics, and ignition can explain the performance of the entire system.

Ignition can depend on physical, chemical, and mixing and transport features of a problem and in some cases on heterogeneous phenomena. Excellent reviews of ignition can be found in current sources [1–4] describing thermal feedback, chemical kinetic chain-branching reactions, and other elements. However, ignition in general is an enormous subject, and the present work cannot provide a thorough treatment.

This paper focuses on chemical kinetic factors in practical systems, with special attention on ignition in automotive engines. Recent advances in experimental and kinetic modeling capabilities have provided new insights into ignition, offering new possibilities for control strategies and new classes of combustors.

General Features of Ignition

Many interesting systems involve chain reactions, such as nuclear reactors, with neutrons as chain carriers. Chain termination is provided by neutron absorbers, and chain branching is associated with the term *supercritical*, normally a condition to be avoided. Populations of living organisms obey the same reactivity laws. Organisms can grow exponentially via chain branching until limited availability of nutrients first stabilizes the population and eventually quenches the system via chain termination.

Reacting systems follow the general equation

$$\frac{dn(t)}{dt} = k\ n(t) \tag{1}$$

where $n(t)$ is the number of chain carriers. This indicates that the change in number of neutrons in a reactor depends on the number of neutrons available to produce further neutrons or the change in the number of bacteria depends on the number of bacteria which can reproduce, a reflection that the current population of chain carriers produces the next generation of chain carriers.

Solution of equation 1 leads to the expression

$$n(t) = n(0)\ \exp(kt) \tag{2}$$

When $k < 0$, the result is exponential decay; when

Report Documentation Page

Form Approved
OMB No. 0704-0188

1. REPORT DATE	2. REPORT TYPE	3. DATES COVERED
04 AUG 2000	**N/A**	**-**

4. TITLE AND SUBTITLE	5a. CONTRACT NUMBER
Chemical Kinetics of Hydrocarbon Ignition in Practical Combustion Systems	5b. GRANT NUMBER
	5c. PROGRAM ELEMENT NUMBER
6. AUTHOR(S)	5d. PROJECT NUMBER
	5e. TASK NUMBER
	5f. WORK UNIT NUMBER
7. PERFORMING ORGANIZATION NAME(S) AND ADDRESS(ES) **Lawrence Livermore National Laboratory Livermore, CA 94550, USA**	8. PERFORMING ORGANIZATION REPORT NUMBER
9. SPONSORING/MONITORING AGENCY NAME(S) AND ADDRESS(ES)	10. SPONSOR/MONITOR'S ACRONYM(S)
	11. SPONSOR/MONITOR'S REPORT NUMBER(S)

12. DISTRIBUTION/AVAILABILITY STATEMENT
Approved for public release, distribution unlimited

13. SUPPLEMENTARY NOTES
See also ADM001790, Proceedings of the Combustion Institute, Volume 28. Held in Edinburgh, Scotland on 30 July-4 August 2000.

14. ABSTRACT

15. SUBJECT TERMS

16. SECURITY CLASSIFICATION OF:			17. LIMITATION OF ABSTRACT	18. NUMBER OF PAGES	19a. NAME OF RESPONSIBLE PERSON
a. REPORT	b. ABSTRACT	c. THIS PAGE			
unclassified	**unclassified**	**unclassified**	**UU**	**15**	

Standard Form 298 (Rev. 8-98)
Prescribed by ANSI Std Z39-18

$k > 0$, the radical population experiences exponential growth. Thus, $k \cong 0$ is equivalent to criticality or steady combustion (or population stability). In a chemically reactive system, the coefficient k is an average over all reactions taking place, including initiation, termination, propagation, and branching reactions. We can define ignition by requiring that the reacting system experience exponential growth in both temperature and number of chain carriers, and the exponential chain reaction must proceed for a significant degree of fuel consumption.

Chain Reactions

Early analyses [5,6] established the chain character of reaction of the H_2-O_2 system, and the same principles apply to hydrocarbon oxidation. Chain carriers are radical species such as H and O atoms, OH, CH_3, and HO_2, and it is usually straightforward to identify reactions as initiation, propagation, branching, and termination.

Initiation reactions generate radicals from stable species, such as the decomposition of propane:

$$C_3H_8 \rightarrow CH_3 + C_2H_5 \qquad (3)$$

Chain propagation reactions maintain the number of radical species, as in

$$C_2H_6 + OH \rightarrow C_2H_5 + H_2O \qquad (4)$$

consuming OH and producing ethyl radicals. Chain termination reduces the number of radicals, as in recombination producing stable butane:

$$C_2H_5 + C_2H_5 \rightarrow C_4H_{10} \qquad (5)$$

The key to understanding ignition kinetics is to identify the chain branching steps under the conditions being studied. In chain branching reactions, the number of radicals increases, as in

$$CH_4 + O \rightarrow CH_3 + OH \qquad (6)$$

consuming one O atom and producing two radicals. The most important high temperature chain branching reaction consumes one H atom and produces two radicals, O and OH:

$$H + O_2 \rightarrow O + OH \qquad (7)$$

These illustrations are encapsulated into single reactions. However, it is common to find situations in which chain properties are best attributed to a sequence of reactions. For example, an important reaction sequence is

$$C_3H_8 + HO_2 \rightarrow C_3H_7 + H_2O_2 \qquad (8)$$

$$H_2O_2 \rightarrow OH + OH \qquad (9)$$

consuming one hydroperoxy radical and producing three radicals, a propyl radical and two hydroxyl radicals. In some situations, the sequence of reactions can be much longer before its chain properties become evident.

Finally, not all radical species have the same influence on the overall reaction rate, due to subsequent reactions with different branching characteristics. For example, at high temperatures, where reaction 7 is the major chain-branching step, production of ethyl radicals accelerates the overall rate of ignition because C_2H_5 produces H atoms, which then provide

$$C_2H_5 \rightarrow C_2H_4 + H \qquad (10)$$

chain branching via reaction 7, while production of methyl radicals actually decreases or inhibits the overall rate of ignition at high temperatures because methyl radicals recombine, resulting in chain termination:

$$CH_3 + CH_3 \rightarrow C_2H_6 \qquad (11)$$

The specific reaction sequences that provide chain branching change as the temperature, pressure, and reactant composition change. In discussions below, chemical kinetic factors for ignition under a variety of conditions will be examined, and, for each environment, the essential task will be to identify the chemical kinetic reaction sequences that lead to chain branching.

High Temperature Ignition, Shock Tubes, Detonations, and Pulse Combustors

At temperatures above about 1200 K, the dominant chain-branching step in hydrocarbon ignition is reaction 7 [7–12], with H atoms that are produced by thermal decomposition of radicals such as ethyl, vinyl, formyl, isopropyl, and others. Activation energies of these reactions are quite large (e.g., 30 kcal/mol), and the activation energy of reaction 7 is also quite large (16.8 kcal/mol), so these reactions need high temperatures to proceed.

Shock Tubes

High temperature ($T \geq 1200$ K) shock tube ignition is controlled by reaction 7. At shock tube temperatures, there is an initiation period for radical generation, followed by a period of explosive, exponential growth in radicals, dominated by reaction 7, consuming fuel and increasing the temperature. An interesting series of experiments was reported by Burcat et al. [13] for ignition of stoichiometric mixtures of *n*-alkanes in oxygen/argon. Fuels included methane, ethane, propane, *n*-butane, and *n*-pentane. Measured ignition delay times are summarized as symbols in Fig. 1, together with computed values using kinetic reaction mechanisms, with the exception of ethane; the heavy dashed line is a fit to the experimental results for ethane ignition,

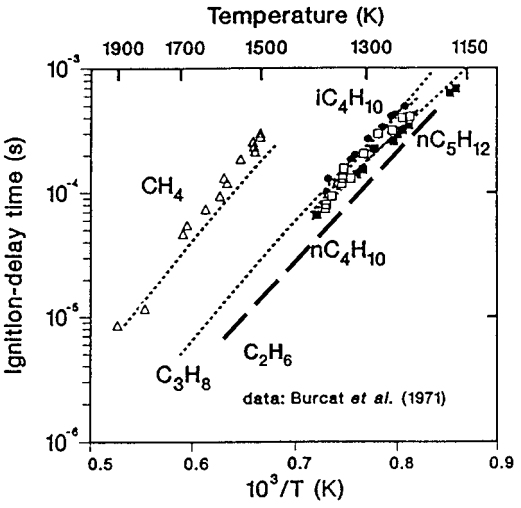

FIG. 1. Ignition delay times for C_1–C_5 alkanes. Experimental data are from Burcat et al. [13]; computed lines are Westbrook and Pitz [10]. The dark dashed line is a fit to the experimental results for ethane ignition from Ref. [13], and no computed results for ethane ignition were carried out. Experimental points: open triangles, methane; filled circles, propane; filled squares, *n*-pentane; open squares, *n*-butane.

and no computed results for ethane are presented in Fig. 1. Calculated results for isobutane are indicated as a dotted line and are virtually indistinguishable from *n*-butane and *n*-pentane. Of these five *n*-alkane fuels, methane ignites slowest, ethane most rapidly, and the three higher *n*-alkanes have intermediate reactivity and are very similar to each other. Kinetic modeling shows that methane ignites slowest because methyl radicals, resulting from H-atom abstraction from methane, lead to chain termination through reaction 11. Ethane is most reactive because every ethyl radical, resulting from H-atom abstraction from ethane, produces an H atom via reaction 10. For higher *n*-alkanes, two or more alkyl radicals are produced, some of which produce H atoms and chain branching through reaction 7 and some of which produce methyl radicals and chain termination through reaction 11. For example, butyl radicals from *n*-butane decompose:

$$1\text{-}C_4H_9 \rightarrow C_2H_4 + C_2H_5 \qquad (12)$$

$$2\text{-}C_4H_9 \rightarrow C_3H_6 + CH_3 \qquad (13)$$

Since reaction 10 produces H atoms from C_2H_5, these two steps show that *n*-butane produces a mixture of H atoms and CH_3 radicals, and the same is true with propane and *n*-pentane. Thus, methane and ethane represent extremes of reactivity, while larger alkane hydrocarbons have intermediate ignition properties due to their mixed production of H and CH_3.

Sensitivity of the high temperature mechanism to reaction 7 is responsible for many practical phenomena. Flame and detonation inhibitors catalyze removal of H atoms [14–19], as illustrated here in the case of HBr:

$$H + HBr \rightarrow H_2 + Br \qquad (14)$$

$$H + Br_2 \rightarrow HBr + Br \qquad (15)$$

$$Br + Br + M \rightarrow Br_2 + M \qquad (16)$$

for a net reaction of

$$H + H \rightarrow H_2$$

This net removal of H atoms reduces the number of H atoms available for chain branching via reaction 7 and slows the overall rate of ignition.

This discussion addresses the most common shock tube experiments. However, some shock tube experiments are carried out at lower temperatures [20] or at significantly elevated pressures [21], where the chain branching reaction sequences are different from the conventional high temperature conditions outlined here; these reaction environments will be discussed below.

Detonations

High temperature ignition kinetics and reaction 7 play essential roles in the propagation of gaseous detonations, where postcompression detonation temperatures and pressures are comparable with those in shock tubes. Although it is often convenient to consider a detonation as a planar phenomenon, detonations have a complex, three-dimensional structure caused by interactions between transverse waves in the reactive medium [22,23]. The reactive shock wave decays during propagation and would fail if new ignition spots were not created by intersecting shock waves, or Mach stems. For this reason, detonation propagation depends very strongly on ignition kinetics. The result of these interactions is a cellular structure that can be measured using smoked foils in laboratory experiments. The widths of these detonation cells are fundamental features relating to the initiation, propagation, and stability of gaseous detonations.

Because detonation structure is inherently three-dimensional, and the reaction zone is spatially thin relative to cell sizes, computer models for detonations [24] have been unable to include full chemical submodels, although recent models [25] have used tabular look-up techniques to include finite-rate kinetics. Advances in massively parallel computer capabilities are likely to permit inclusion of detailed kinetics in future three-dimensional CFD models of detonations.

Given the computer costs of a three-dimensional detonation model, the pseudo–one-dimensional

Zeldovich-von Neumann-Döring (ZND) model [26–28] has been used to relate computed ignition delay times to characteristic spatial and energy scales in a detonation. This approach calculates ignition delay times behind a Chapman-Jouguet (CJ) shock wave to define a characteristic length scale in the reacting gas mixture [29–37], which is then proportional to the cell width, critical tube diameter, minimum initiation energy, and other detonation characteristics.

An exciting current development is extension of kinetic modeling to study detonations of condensed phase explosives [38–41], such as ammonium perchlorate, RDX, or HMX. These models require treatment of three-dimensional fluid mechanics, multiphase phenomena, and detailed chemical kinetics, and massively parallel computing is an essential computational tool. Ignition kinetics in such an environment are complex, and a great deal of new research is needed.

Pulse Combustion

Pulse combustion has been known for centuries, but only recently have its physical and chemical principles become understood. Ignition and heating in the pulse combustor force exhaust gases out through an exhaust pipe; the resulting lower pressure in the combustion chamber then draws in fresh fuel and air. This fresh mixture combines with hot residual products of the previous burn, and the resulting fresh reactants and residual gases ignite, starting a new cycle. Because the average temperature is relatively low, production of NO_x is also low.

Keller et al. [42–45] examined mixing, kinetics of ignition, and resonant acoustic wave propagation in the pulse combustor, showing that ignition must be timed to occur in phase with resonant pressure waves in the combustion chamber.

The kinetic submodel for this system mixes fresh fuel and air, initially at room temperature, with hot residual gases from the preceding cycle, steadily increasing the temperature of the fresh mixture as well as diluting it with the residual products. The overall reaction rate remains negligible until the mixture reaches temperatures of about 1200 K, where ignition is controlled by reaction 7. The kinetic model for this system predicts the influence of additives and variability in natural gas composition [46] to manipulate the kinetics of ignition in a pulse combustor. This is a very rich system in terms of the parameters that can be adjusted to optimize the phasing between kinetic ignition and the resonant pressure wave in the combustion chamber. In addition to the kinetic parameters, the combustion chamber acoustic timescales can be modified, and the mixing rate can be varied by adjusting intake ports for fuel and air.

Intermediate Temperature Ignition, Rapid Compression Machines, Engine Knock, Diesel Ignition, and Homogeneous Charge, Compression Ignition (HCCI)

At temperatures above about 850 K but below 1200 K, reaction 7 is too slow to provide sufficient branching rates for ignition, and a different reaction path dominates. Key reactions include the following:

$$H + O_2 + M \rightarrow HO_2 + M \quad (17)$$

$$RH + HO_2 \rightarrow R + H_2O_2 \quad (18)$$

$$H_2O_2 + M \rightarrow OH + OH + M \quad (19)$$

where RH is an alkane, R is an alkyl radical, and M is a third body. Collectively, reactions 17–19 consume one H-atom radical and produce two OH radicals, providing chain branching.

Kinetic studies in flow reactors and stirred reactors [47–49] at temperatures of about 1000 K show that reactions 17–19 control combustion rates. In this range, reaction 19 is rapid, so H_2O_2 decomposes as rapidly as it is formed and H_2O_2 concentrations do not build up to appreciable levels. However, in many practical systems, the dominant feature of ignition is the accumulation of H_2O_2 until a temperature is reached where it decomposes to cause ignition. This is true in the laboratory rapid compression machine, and it is also the central kinetic feature in engine knock in spark ignition engines, in ignition in liquid-fueled diesel engines, and in the operation of homogeneous charge, compression ignition (HCCI) engines. In each of these systems, H_2O_2 forms at lower temperatures and remains relatively inert, until increasing temperature from compression and exothermic reactions reaches a level where it decomposes rapidly via reaction 19. Each of these examples will be discussed below.

Rapid Compression Machine

Rapid compression machines (RCMs) have been used for many years [50–52] and provide a fertile environment for the study of hydrocarbon oxidation. The apparatus provides a combustion chamber with a single piston stroke, leaving the compressed gases at temperatures from 550 to 950 K, depending on the compression ratio of the RCM and specific heats of reactant gases. Compressed gases can undergo a single-stage or two-stage ignition, or the reactants may not ignite at all while heat transfer cools the mixture to room temperature.

Typical results in Fig. 2 are taken from numerical simulation of ignition of a stoichiometric mixture of neopentane and oxygen in N_2 and Ar in proportions of $C_5H_{12}/O_2/N_2/Ar = 0.0256/0.2048/0.38/0.39$ at a postcompression temperature of 757 K [53]. In this example, the temperature history shows a well-defined two-stage ignition, the first stage occurring after a delay of 5 ms, reaching a new temperature of

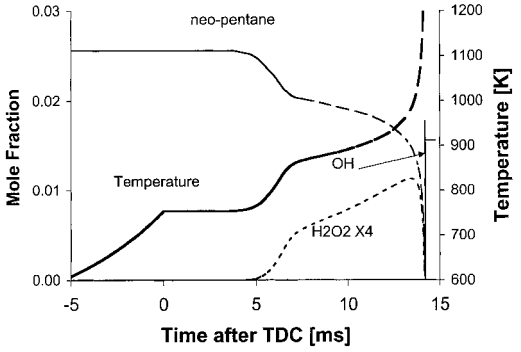

FIG. 2. Computed temperature and concentrations of neopentane, H_2O_2, and OH from Ribaucour et al. [53].

about 880 K. The temperature then remains relatively constant, rising slowly for the next 6–8 ms, then rising more rapidly until a total elapsed time of 14 ms, when the second-stage ignition is observed and the temperature rises rapidly, consuming all of the fuel. In other cases, the first stage can occur during the compression stroke [54,55] and is completed before the end of the compression, while in other cases there is no discernible first-stage ignition.

The first-stage ignition is a result of rather complex kinetic features of low temperature hydrocarbon oxidation [56]. This regime has considerable importance in theoretical and practical systems, and we will return to describe it in more detail below.

Figure 2 plots the concentrations of fuel, H_2O_2, and OH. During the time preceding the second-stage ignition, H_2O_2 concentration increases steadily. Until the temperature approaches 1000 K, decomposition of H_2O_2 is much slower than its production, and the small amounts of OH produced are consumed by reactions with the fuel [57]. When a temperature close to 1000 K is reached, reaction 19 accelerates, H_2O_2 disappears, and OH concentration increases rapidly. The increased OH concentrations rapidly consume any remaining fuel, followed by a rapid increase in temperature. Thus, decomposition of H_2O_2 and consumption of fuel result in ignition.

There is a critical temperature for ignition through H_2O_2 decomposition that is a function of the pressure of the reactive system. This is seen by examining the rate of H_2O_2 decomposition

$$\frac{d[H_2O_2]}{dt} = -[H_2O_2]\ [M]k \qquad (20)$$

where M is the total molar concentration. This equation can be rearranged into the form $[H_2O_2]/(d[H_2O_2]/dt)$; a characteristic decomposition time is

$$\tau = [H_2O_2]/(d[H_2O_2]/dt) = 1/(k[M]) \qquad (21)$$

With the rate constant for reaction 19, $k_{19} = 1.2 \times 10^{17} * \exp(-45{,}500/RT)$, τ becomes

$$\tau = 8.3 \times 10^{-18} * \exp(+22{,}750/T) * [M]^{-1} \qquad (22)$$

As the temperature increases, τ becomes smaller, and when it is "short" compared with the residence time, ignition occurs. Characteristic decomposition time also decreases with increasing total concentration [M] or with increasing pressure at constant temperature. Therefore, as pressure increases, the critical temperature for ignition decreases gradually.

Total postcompression concentrations in a representative RCM experiment are 1×10^{-4} mol/cm^3, so τ is approximately 7.8 ms at $T = 900$ K, 640 μs at $T = 1000$ K, and 80 μs at $T = 1100$ K. With total reaction times of tens of milliseconds, rapid decomposition is observed at about 950–1000 K, with characteristic times for ignition less than a millisecond. In studies of ignition at the higher pressures of internal combustion engines, including spark ignition, diesel, and HCCI engines, the same calculation of equations 20–22 shows that this simple mechanism predicts ignition at temperatures between 900 and 950 K [58]. Analysis of reaction 19 by Griffiths and Barnard [1] at its high pressure limit shows similar rates of decomposition at somewhat lower temperatures, consistent with the above trends as pressure increases.

The key is that H_2O_2 decomposes rapidly at temperatures of 900–1000 K, so this temperature can be considered as a critical value in systems in which the temperature approaches this value from lower temperatures. H_2O_2 is produced at lower temperatures by low and intermediate temperature kinetic pathways, until the decomposition temperature is reached, when the system suddenly produces large numbers of OH radicals and rapidly ignites. The most important variable is the time at which they reach this critical temperature. Anything that will accelerate reaching this critical temperature advances its ignition, while delaying it inhibits ignition. The importance of the first-stage, low temperature oxidation period is that it provides heat release early in the reaction history, so the reactive mixture arrives at the decomposition temperature earlier than would have occurred without that early heat release.

Low Temperature Chemical Kinetics

Low temperature hydrocarbon oxidation has been studied extensively [56]. Following abstraction of H atoms from the fuel, at high temperatures the alkyl radical R decomposes, producing olefin and smaller alkyl radicals, and reaction 7 is the dominant chain-branching reaction, as discussed above. At lower temperatures, O_2 adds to the alkyl:

$$R + O_2 + M \rightarrow RO_2 + M \qquad (23)$$

The equilibrium constant for reaction 23 is strongly

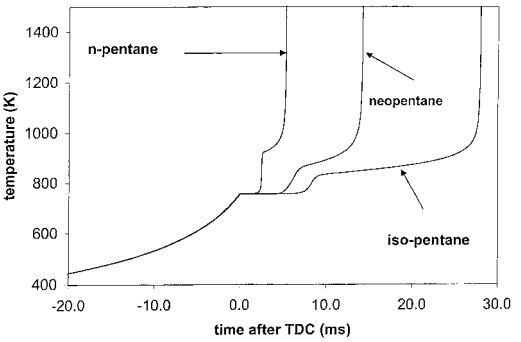

FIG. 3. Computed temperatures in ignition of the three isomers of pentane, from Ribaucour et al. [53].

temperature dependent and is strongly in favor of RO_2 at low temperature, shifting toward R + O_2 as the temperature increases. RO_2 radicals isomerize to produce a QOOH radical species

$$RO_2 \rightarrow QOOH \quad (24)$$

Isomerization depends sensitively on the size and structure of the original fuel molecule and the site in that fuel where the O_2 group is located [56,58]. The RO_2 will be produced with excess energy, so it is important to understand the rate of collisional stabilization and whether subsequent reactions occur from the activated or ground state of RO_2. The simplest example of such a system is the ethyl radical, with RO_2 being the ethylperoxy radical $C_2H_5O_2$ and QOOH being the hydroperoxyethyl radical C_2H_4OOH. This system has been studied extensively [59–63], and even this small system is not fully understood. Bozzelli and Pitz [64] and Koert et al. [65] examined the propyl + O_2 system, but little experimental or theoretical work has been done for larger systems.

Several factors influence the rate of internal H-atom transfer or radical isomerization. The species forms a ringlike transition state where the terminal O atom approaches an extractable H atom within the RO_2 species. The number of atoms in this transition state ring influences the rate of reaction, with six- and seven-membered rings having the most rapid rate. The type of C-H bond broken has a strong influence, with primary C-H bonds being strongest, secondary C-H bonds next, and tertiary C-H bonds being weakest. The rate and number of possible RO_2 isomerization reactions increase with the fuel molecule size and are fastest in long, linear alkane fuel molecules, with a large number of six- and seven-membered transition state rings and a high percentage of easily abstracted secondary C-H bonds, and are slowest in highly branched fuel molecules, with fewer low-energy transition state rings and large percentages of difficult-to-abstract primary C-H bonds [58].

QOOH species react via several alternative paths which are formally chain propagation steps,

$$QOOH \rightarrow Q + HO_2 \quad (25)$$

$$QOOH \rightarrow QO + OH \quad (26)$$

beginning with one alkyl radical, and produce one HO_2 or OH radical, in addition to a stable olefin or cyclic ether. However, it is also possible for a second O_2 molecule to add to QOOH, creating a radical O_2QOOH, which can then isomerize further

$$QOOH + O_2 \rightarrow O_2QOOH \quad (27)$$

again with rates dependent on the structure and size of the original fuel molecule, as observed for RO_2 isomerization. The isomerized product decomposes into a relatively stable ketohydroperoxide species and one OH radical. The ketohydroperoxide species then has its own temperature for decomposition at about 800 K, somewhat lower than that of H_2O_2. Upon reaching this temperature, the ketohydroperoxide decomposes into several pieces, at least two of which are radicals. Thus, it is not until this final ketohydroperoxide decomposition step that chain branching is finally achieved in the low temperature oxidation regime. Since at least three of the ultimate products of this reaction sequence are radicals, chain branching is quite strong once the ketohydroperoxide decomposes. Production of metastable intermediates, ketohydroperoxide in this case and H_2O_2 earlier, followed later by the higher temperature decomposition of the metastable intermediate to finally provide chain branching are examples of degenerate chain branching. Detailed low temperature reaction mechanisms have been developed [53–55,58,66,67] for a variety of hydrocarbon fuels.

This highly branched, low temperature oxidation phase continues until the temperature has increased enough that the equilibria in the molecular oxygen addition reactions 23 and 27 begin to shift toward dissociation. Because activation energies for dissociation are large (i.e., ~35 kcal/mol), the reactions shift rapidly toward dissociation as temperature increases. This shift with hydrocarbon fuels occurs at temperatures near 850 K. The temperature above which these equilibria favor dissociation has been termed the "ceiling temperature" by Benson [68,69].

The effect of fuel molecular structure on both the first- and second-stage ignition is illustrated in Fig. 3, from Ribaucour et al. [53]. The three isomers of pentane are compared at the same postcompression temperature of 757 K. All three mixtures ignite at about 950 K. *n*-pentane ignites first since its first stage occurs first and provides the largest temperature increase, neopentane (2,2-dimethyl propane) ignites next, and isopentane (2-methyl butane) is last, all because the time of occurrence and temperature increase of the first-stage ignition vary in

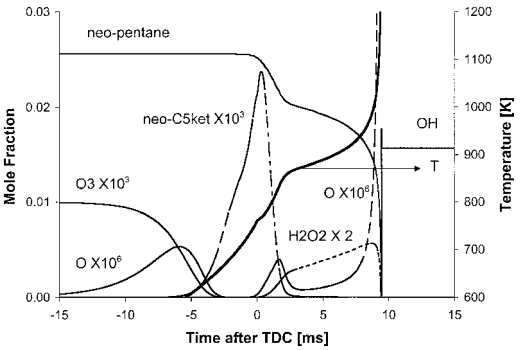

FIG. 4. Computed temperature and selected species concentrations from rapid compression machine ignition of neopentane. Same initial conditions as Fig. 2, but with 10 ppm ozone included.

that order. All ignite when they reach the same critical temperature for H_2O_2 decomposition, and the differences between the isomers are the times when the fuel mixtures reach the critical temperature.

Total heat release in this low temperature regime is quite modest. In Fig. 3, this varies from 50 K for 2-methyl butane to 150 K for *n*-pentane. In engine studies, at top dead center (TDC) this difference makes a significant impact on ignition properties of the combustion system.

An interesting variation of this analysis simulates an RCM experiment in which an additive has been included in the neopentane fuel. This additive, ozone, has an initial concentration of 10 ppm and decomposes early in the experimental cycle, since the activation energy for ozone decomposition is 24 kcal/mol, much less than the 45.5 kcal/mol for H_2O_2 decomposition. Repeating the analysis of equations 20–22, the critical decomposition temperature for ozone at present conditions is about 600 K. Computed results of this example are shown in Fig. 4.

Decomposition of ozone at 5 ms before TDC (at ~600 K) produces O atoms. Each O atom consumes two fuel molecules

$$O_3 + M \rightarrow O_2 + O + M \qquad (28)$$

$$C_5H_{12} + O \rightarrow C_5H_{11} + OH \qquad (29)$$

$$C_5H_{12} + OH \rightarrow C_5H_{11} + H_2O \qquad (30)$$

Pentyl radicals then proceed via reactions 23–27 and produce the metastable C_5 ketohydroperoxide species, the production of which is shown in Fig. 4, immediately following the decomposition of ozone.

Ketohydroperoxide decomposition has an activation energy of about 42 kcal/mol, so it decomposes at about 800 K, as seen in Fig. 4. Production of OH from decomposition produces further water and heat release. Decomposition of H_2O_2 and the ketohydroperoxide and the resulting heat release bring the reactive mixture to the first ignition stage before the conclusion of the compression stroke. Fig. 4 shows a slight inflection point at TDC, indicating that the low-temperature ignition is well under way as the compression stroke ends. This phase stops at about 850 K, the same temperature at which the first stage ended in the original mixture, without ozone (Figs. 2 and 3). The kinetics of the first stage have not been altered by the additive, but the time at which it begins was advanced by adding ozone, which stimulated early heat release.

The major intermediate being produced is still H_2O_2, and it still decomposes at 950–1000 K, producing the real ignition. The ozone additive advances the time of ignition from about 14 ms after TDC to about 9 ms after TDC. The second-stage ignition is the same in both cases, but the addition of ozone makes that mixture reach the ignition temperature at an earlier time. Finally, note the peak in O-atom concentration that occurs at each of the three stages of ignition, at times of -6, $+1$, and $+9$ ms after TDC.

Engine Knock

In spark ignition engines, thermodynamic combustion efficiency increases with engine compression ratio. However, an increased compression ratio eventually results in engine knock, limiting engine efficiency in practical engines. Numerical studies have used reduced [70–74] and detailed [66,74–78] kinetic models to understand chemical factors responsible for knock.

In a spark ignition engine, a flame propagates through a combustion chamber, starting at the point of spark ignition. Some reactant gases in the combustion chamber will naturally be the last to be consumed by the flame, termed the *end gases.* End gas conditions are determined by piston motion and combustion in the engine chamber. As piston motion and flame propagation proceed, end gases see increasing levels of pressure and temperature and react accordingly. If end gases reach the point of ignition before being consumed by the flame, knocking behavior will be observed. Mixtures that react more rapidly are more susceptible to knock, while mixtures that ignite more slowly resist knock. Increasing the engine compression ratio increases the rate of autoignition while having little effect on flame propagation, so this increases the potential for knocking behavior. Thus, engine knock is essentially an ignition problem.

Computational modeling of autoignition at engine conditions shows the same features as described for the rapid compression machine. This can be illustrated by examining the way that fuel composition and molecular size and structure influence autoignition behavior and tendency to knock by simulating the critical compression ratio. Experiments were

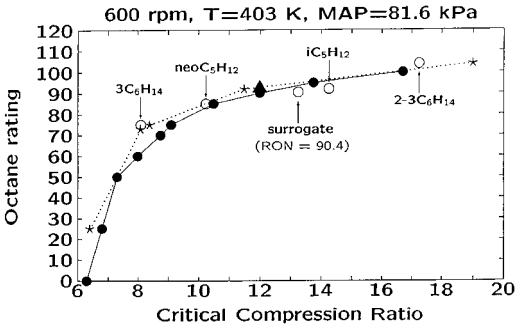

FIG. 5. Correlation of computed critical compression ratio with research octane numbers. Solid circles are primary reference fuel mixtures, other symbols are isomers of hexane and pentane, and stars are experimentally measured values [66].

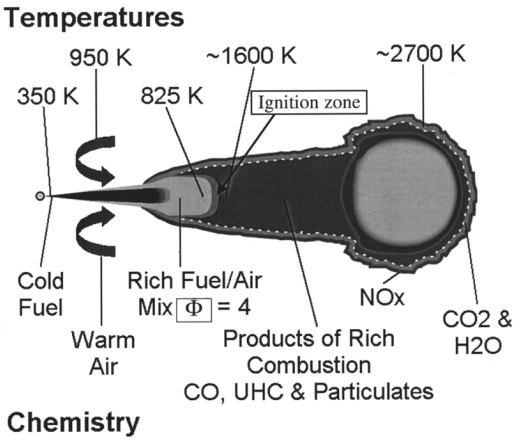

FIG. 6. Schematic model of diesel spray combustion, based on the work of Dec [83]. The ignition region is identified, and the temperatures of the different regions in the combusting spray are noted.

carried out in a Cooperative Fuels Research engine at a low engine speed of 600 rpm and intake manifold temperature of 403 K. These are essentially the same conditions as those in standardized tests for research octane number (RON). For stoichiometric fuel/air mixtures, the engine compression ratio is steadily increased until autoignition is observed. A series of such experiments were carried out by Leppard [79] for a range of alkane and primary reference fuel mixtures, and a kinetic model was used to simulate those experiments [66,72]. Computed and experimental critical compression ratio results are plotted in Fig. 5, together with the measured RONs of each fuel. A rather smooth curve results, although it is clearly not a straight line, indicating that octane rating is a rather nonlinear scale.

A numerical experiment can be carried out to use this information to construct a fuel mixture with an arbitrary octane rating. For example, to create a fuel with a RON of 90.8, a motor octane number (MON) of 83.9, and an overall octane rating (RON + MON)/2 of 89, to compare with ordinary gasoline, a mixture of two isomers of hexane and two isomers of pentane was defined in terms of their individual RON and MON values. These four fuel components are indicated by the arrows in Fig. 5. When tested numerically, this mixture had a critical compression ratio corresponding to a RON of 90.4, very close to the blending value, as shown in Fig. 5.

A critical feature of these computed histories is that they reach peak compression temperatures that are all very nearly the same. Considerable differences in octane number result in only a few degrees of temperature at TDC, resulting in a considerable difference in time of ignition and demonstrating that the octane number scale is highly nonlinear.

Just as observed in the RCM results, these computed results indicate that ignition in each of these cases occurs when H_2O_2 decomposes. Differences in octane number are reflected in small differences in cool flame heat release, with greater amounts of low temperature heat release and higher quantities of H_2O_2 correlating with earlier ignition and lower octane values. Similar conclusions were obtained by Blin-Simiand et al. concerning the central role of H_2O_2 decomposition and its role in autoignition [80].

The effects of various antiknock compounds can be understood in this same framework. Additives including tetraethyl lead, now no longer used, provide kinetic sinks for HO_2 [58,81,82], greatly reduce the production of H_2O_2, and interfere with the intermediate temperature ignition process. Other additives, including methyl *tert*-butyl ether, act by interfering with low temperature oxidation [18,58], reducing the amount of low temperature heat release and retarding the time at which the end gas reaches the H_2O_2 decomposition temperature.

Diesel Ignition

Diesel engines have existed for many years, but until recently many of the basic physical and chemical principles of diesel combustion had not been well understood. Recently, in a series of insightful laser diagnostic studies, Dec provided a coherent, self-consistent picture of diesel combustion [83]. His results, summarized in Fig. 6, show that the fuel jet vaporizes rapidly and mixes with hot, compressed air. The air steadily reduces the fuel/air equivalence ratio at the same time that it is increasing the mixture temperature, and the mixture begins to react. In Dec's observations, this mixture eventually ignites while the equivalence ratio is still quite high ($\phi \approx 4$).

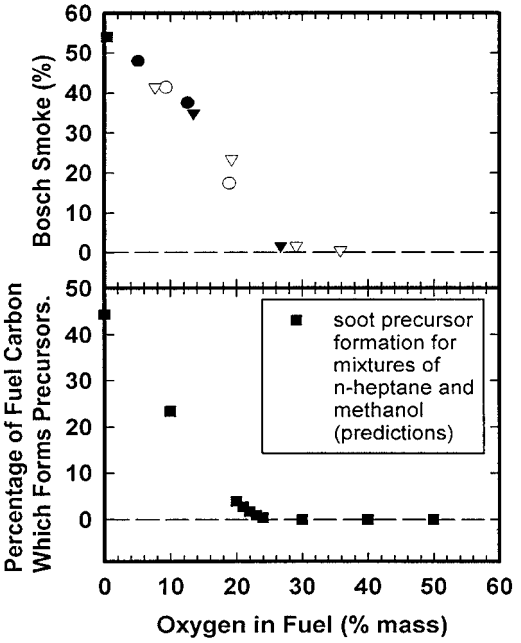

FIG. 7. Experimentally observed variation in Bosch smoke number with fuel oxygenate content, from Miyamoto et al. [90], and variation in computed soot precursor concentrations with fuel oxygenate content, from Flynn et al. [84].

Soot production was observed to proceed immediately from the products of this rich, premixed ignition, and soot was consumed in a diffusion flame at the periphery of the downstream cloud.

This large-scale ignition problem has been analyzed using detailed chemical kinetics [84]. The premixed region begins to react when the local equivalence ratio reaches $\phi \approx 10$, although the rate of reaction is initially quite slow. As air mixes and the mixture temperature increases, the rate of reaction increases. Rapid reaction begins when the mixture temperature reaches about 700 K. As noted above for other classes of applications, this low temperature reaction produces H_2O_2 and produces a modest amount of heat release and temperature increase. Eventually, the mixture reaches the temperature at which H_2O_2 decomposes and ignition is observed. Thus, the kinetic mechanism of diesel ignition is identical to that of the RCM and that of engine knock in spark ignition engines. The major differences occur because diesel ignition takes place under very fuel-rich conditions.

Diesel ignition improvers [85] are species such as ethyl-hexyl nitrate that decompose at temperatures much lower than the ignition temperature provided by H_2O_2 decomposition. Radicals produced by decomposition of the additive consume some fuel and release some heat, raising the temperature of the premixed gases and getting them closer to the H_2O_2 decomposition temperature. Other additives that decompose at lower temperatures and provide radicals would also be effective diesel ignition improvers or cetane improvers. The example of ozone discussed earlier for the RCM would enhance diesel ignition in this same manner.

An especially interesting additional feature of this premixed ignition is the observation by Dec that the products of the rich premixed ignition immediately begin the process of soot precursor and soot production. In computed models of this rich premixed ignition [84], the products of the ignition are the same species that have been shown [86–89] to preferentially produce small aromatic ring species such as benzene, toluene, and naphthalene. Small aromatic species then react to produce larger polycyclic aromatic species and eventually soot. It was shown experimentally [90] that addition of oxygenated species to the fuel can reduce soot emissions in diesel combustion, and this trend was reproduced by kinetic modeling [84] by correlating the total product concentrations of aromatic formation precursors with the amounts of these simple species that survive the premixed rich ignition stage. Thus, soot production is directly related to ignition kinetics in the diesel engine.

Figure 7 shows concentrations of soot produced in diesel engines with the relative amounts of oxygenates in the fuel from the experimental work of Miyamoto et al. [90]. Also shown is the total concentration of ethene, acetylene, and propargyl radical, summed together, to roughly produce a curve similar to that derived experimentally by Miyamoto et al. These modeling calculations [84] were carried out for a variety of oxygenated species (i.e., methanol, ethanol, dimethyl ether, dimethoxy methane, and methyl butanoate) added to *n*-heptane; *n*-heptane is a realistic surrogate diesel fuel with a cetane number of 56. This work suggests strongly that rich premixed ignition does indeed produce the seeds of soot formation and that lowering the postignition concentrations of these elementary species effectively reduces soot production. The sequence of fuel/air mixing, rich premixed ignition, and production of soot precursors, followed eventually by soot burnout, provides a framework for diesel combustion in which each of the detailed steps leads very naturally and continuously to the next step.

Homogeneous Charge, Compression Ignition

Combustion in reciprocating engines under HCCI conditions is an intriguing technology that may offer the opportunity to eliminate NO_x emissions from engine combustion. Particulate emissions are also observed to be very low. Disadvantages are high unburned hydrocarbon and CO emissions, along with high peak pressures and high rates of heat release.

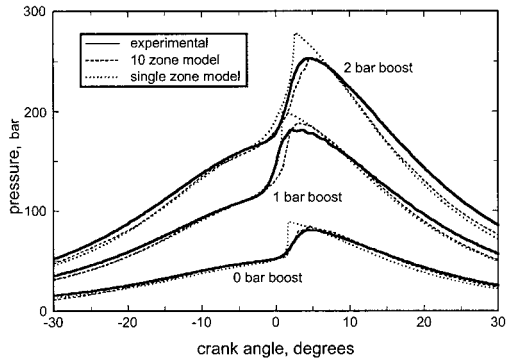

FIG. 8. Comparison between experimental pressure traces [101] and calculated values, using both a single-zone and a 10-zone modeling treatment [98], for three natural gas experiments at different boost pressures.

In an HCCI engine, a premixed, very lean mixture of fuel and air is drawn into the engine chamber and compressed by a piston. Near TDC, the majority of the charge in the engine ignites homogeneously. The time of ignition can be varied by changing the compression ratio, fuel/air equivalence ratio, time of intake valve opening, and intake manifold temperature.

HCCI was identified as a distinct combustion phenomenon about 20 years ago. Initial studies [91–93] recognized the basic characteristics of HCCI; ignition occurs at many points simultaneously, with no flame propagation. It is controlled primarily by chemical ignition kinetics, with little influence from effects such as turbulence or mixing that play such a large role in other engine combustion problems. Simplified kinetics models have been used to analyze HCCI combustion, coupled usually to multidimensional CFD models [94–98], with limited success.

Recently, detailed kinetic modeling was used to examine HCCI combustion [98–100]. For a number of practical fuels, including natural gas, propane, and others, model calculations have reproduced the onset of ignition in good agreement with experimental results carried out at the Lund Institute of Technology [101,102], using a spatially homogeneous model. The product temperature is kept low by operating at very lean conditions, so temperatures are too low to produce significant NO_x emissions. However, a one-zone, homogeneous treatment produces much too rapid a combustion duration, as shown in Fig. 8, and cannot predict CO and hydrocarbon emissions.

HCCI engine wall temperatures are low, so there is an extensive engine chamber thermal boundary layer, and not all the boundary layer fuel burns together with the initial bulk ignition. In addition, there is unburned fuel in the piston ring and other crevice volumes that does not burn immediately. Since the peak bulk temperatures are low and decrease further after TDC, most fuel in the boundary layer and crevices cannot diffuse out into the bulk gas and burn; this material is ultimately exhausted without further reaction. However, some fraction of these gases can be partially burned, resulting in products of incomplete combustion and especially CO.

A full kinetic, spatially varying model [99] can account for the temperature distribution in the boundary layer and crevices, in addition to the main bulk charge, to predict unburned hydrocarbon and CO emissions from this engine. As a result of this varying temperature distribution in the fuel/air mixture, the overall heat release is spread out in time relative to the one-zone homogeneous treatment, in much better agreement with experimental results, as shown in Fig. 8 for cases in which the bulk region and boundary layer were defined by 10 spatial zones.

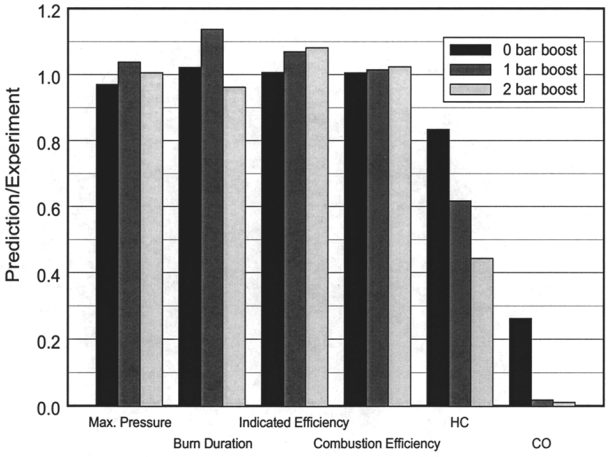

FIG. 9. Ratios of experimental [101] to numerical results [98] for the main combustion parameters of HCCI, for natural gas at different boost pressures, using the 10-zone spatial model.

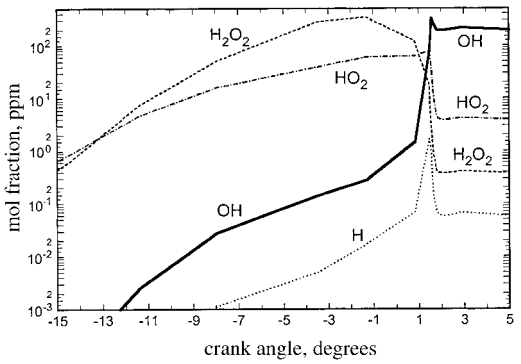

FIG. 10. Computed concentrations of basic species in parts per million in the bulk gases in HCCI ignition, with natural gas fuel [98].

This more refined model describes many experimental features of HCCI very well except for the predicted CO emissions, as shown in Fig. 9.

The kinetic details of these model computations indicate that HCCI ignition is controlled by H_2O_2 decomposition. Computed variations in selected species concentrations are summarized in Fig. 10, in which it is clear that H_2O_2 decomposition occurs at the time of autoignition, observed experimentally [100] to occur at about 1° after TDC. The fuel/air mixture follows a temperature and pressure history very similar to those encountered by end gases in spark ignition engines and in a rapid compression machine. Modest heat release occurs at lower temperatures, depending on the cool flame reactivity of the specific fuel or fuel mixture, resulting in variable amounts of early temperature increase. Variation in any engine parameter that gets the reactive fuel/air mixture to the H_2O_2 decomposition temperature of about 1000 K earlier will advance ignition, and anything that delays reaching that temperature will retard ignition. Increasing the intake manifold temperature and use of proignition additives such as ozone (see Fig. 4) or ethyl-hexyl nitrate advance ignition, while exhaust gas recirculation and addition of knock suppressants retard ignition.

In many ways, HCCI combustion is very simple. Low and intermediate temperature reaction sequences process the fuel/air mixture during its compression; the amount of low temperature, cool flame heat release varies, depending on the composition of the fuel. Ignition occurs at the temperature where the core fuel/air charge reaches the H_2O_2 decomposition temperature, so models developed for engine knock and rapid compression machines are directly applicable to HCCI systems. Low NO_x production is a result of the very low overall fuel/air equivalence ratio; the low equivalence ratio is possible because flame propagation is not required in the HCCI engine [103]. Combustion is spread out in time because the extended boundary layer reacts later than the core gases. High hydrocarbon and CO emissions are an inevitable result of the low bulk gas temperatures and wall boundary layers, and it is very likely that postcombustion exhaust gas treatments will be necessary to make HCCI combustion viable. If low temperature hydrocarbon catalysts were to become available, HCCI would represent an important competitor to conventional spark ignition and diesel engines.

Summary

The role of chain branching in determining the onset of ignition has identified two distinct chain-branching mechanisms affecting hydrocarbon ignition in practical systems. The high temperature (above ~1200 K) mechanism is important in shock tube ignition and practical systems including detonations and pulse combustors. These are primarily thermal ignitions, where heat release increases the temperature, further increasing the rate of ignition until reactant depletion ends the ignition.

The second chain-branching regime depends on H_2O_2 decomposition at about 900–1000 K. Experiments in rapid compression machines and flow reactors and corresponding model calculations confirm the importance of H_2O_2 decomposition kinetics and provide insight into the mechanisms of ignition. When these models are then applied to practical systems, especially in engine environments, it is clear that the same kinetic features control ignition in all of these systems. Modifications of the combustion environment that enable a system to reach the decomposition temperature at earlier times advance ignition, while modifications that delay reaching that temperature retard ignition.

This analysis shows that autoignition in engines is dominated by only one elementary reaction, H_2O_2 decomposition. Low temperature reactions or cool flames, including the highly chain branched alkylperoxy radical isomerization kinetic system, simply advance the time at which H_2O_2 decomposition is observed. This simplifies the analysis of combustion ignition phenomena and focuses kinetic attention on a very limited family of reactions that control autoignition phenomena in a very wide range of practical systems.

Acknowledgments

The many contributions of colleagues are gratefully noted, including those of Bill Pitz, Henry Curran, Fred Dryer, Bill Leppard, Nick Marinov, Nick Cernansky, John Griffiths, Jürgen Warnatz, Jim Miller, Pat Flynn, Bengt Johansson, Magnus Christensen, and many others who have provided experimental data, theoretical insight, hard work, and encouragement. Kinetic modeling is a collaboration in

many ways, and the insights provided by the present work are the collective product of all of these individuals. This work has been carried out under the auspices of the U.S. Department of Energy by University of California Lawrence Livermore National Laboratory under contract W-7405-Eng-48.

REFERENCES

1. Griffiths, J. F., and Barnard, J. A., *Flame and Combustion,* Chapman and Hall, London, 1995.
2. Laidler, K. J. *Chemical Kinetics, 3rd ed.,* Harper and Row, New York, 1987.
3. Glassman, I., *Combustion,* Academic Press, New York, 1977.
4. Bowes, P. C., *Self-Heating: Evaluating and Controlling the Hazard,* HMSO Books, London, 1984.
5. Semenov, N. N., *Chemical Kinetics and Chain Reactions,* Oxford University Press, Oxford, U.K., 1935.
6. Hinshelwood, C. N., *The Kinetics of Chemical Change,* Clarendon Press, Oxford, 1940.
7. Frenklach, M., Wang, H., and Rabinowitz, M. J., *Prog. Energy Combust. Sci.* 18:47–73 (1992).
8. Westbrook, C. K., *Combust. Sci. Technol.* 20:5–17 (1979).
9. Warnatz, J., *Proc. Combust. Inst.* 18:369–384 (1981).
10. Westbrook, C. K., and Pitz, W. J., in *Shock Waves and Shock Tubes,* (D. Bershader and R. Hanson, eds.) Stanford University Press, Stanford, CA, 1986.
11. Yetter, R. A., Dryer, F. L., and Rabitz, H., *Combust. Sci. Technol.* 79:97–128 (1991).
12. Curran, H. J., Simmie, J. M., Dagaut, P., Voisin, D., and Cathonnet, M., *Proc. Combust. Inst.* 26:613–620 (1996).
13. Burcat, A., Scheller, K., and Lifshitz, A., *Combust. Flame* 16:29–33 (1971).
14. Dixon-Lewis, G., *Combust. Flame* 36:1 (1979).
15. Westbrook, C. K., *Combust. Sci. Technol.* 23:191–202 (1980).
16. Westbrook, C. K., *Proc. Combust. Inst.* 19:127–141 (1983).
17. Moen, I. O., Ward, S. A., Thibault, P. A., Lee, J. H., Knystautas, R., Dean, T., and Westbrook, C. K., *Proc. Combust. Inst.* 20:1717–1725 (1985).
18. Gray, J. A., and Westbrook, C. K., *Int. J. Chem. Kinet.* 26:757–770 (1994).
19. Westbrook, C. K., *Combust. Sci. Technol.* 34:201–225 (1983).
20. Ciezki, H. K., and Adomeit, G., *Combust. Flame* 93:421–433 (1993).
21. Davidson, D. F., Petersen, E. L., Rohrig, M., Hanson, R. K., and Bowman, C. T., *Proc. Combust. Inst.* 26:481–488 (1996).
22. Strehlow, R. A., *Combust. Flame* 12:81–101 (1968).
23. Nettleton, M. A., *Gaseous Detonations, Their Nature, Effects and Control* Chapman and Hall, New York, 1987.
24. Taki, S., and Fujiwara, T., *Proc. Combust. Inst.* 18:1671–1681 (1981).
25. Kailasanath, K., Oran, E. S., Boris, J. P., and Young, T., *Combust. Flame* 61:199–209 (1985).
26. Zeldovich, Ya. B., *J. Exp. Theor. Phys. USSR* 10:524 (1940).
27. von Neumann, J., *Progress Report on the Theory of Detonation Waves,* OSRD rept. 549, 1942.
28. Döring, W., *Ann. Phys.* 43:421 (1943).
29. Atkinson, R., Bull, D. C., and Shuff, P. J., *Combust. Flame* 39:287 (1980).
30. Westbrook, C. K., *Combust. Flame* 46:191–210 (1982).
31. Westbrook, C. K., *Combust. Sci. Technol.* 29:67–81 (1982).
32. Westbrook, C. K., *Proc. Combust. Inst.* 19:127–141 (1983).
33. Westbrook, C. K., and Urtiew, P. A., *Proc. Combust. Inst.* 19:615–623 (1983).
34. Westbrook, C. K., and Urtiew, P. A., *Fizika Goreniya y Fizryva* 19(6):65–76 (1983).
35. Shepherd, J., *AIAA Progress in Astronautics and Aeronautics: Dynamics of Reactive Systems, vol. 106* (J. R. Bowen, J.-C. Leyer, and R. I. Soloukhin, eds.) AIAA, New York, pp. 263–293.
36. Matsui, H., and Lee, J. H. S., *Proc. Combust. Inst.* 17:1269–1280 (1979).
37. Tieszen, S. R., Stamps, D. W., Westbrook, C. K., and Pitz, W. J., *Combust. Flame* 84:376–390 (1990).
38. Melius, C. F., in *Chemistry and Physics of Energetic Materials,* Kluwer, Netherlands, 1990, pp. 51–78.
39. Yetter, R. A., Dryer, F. L., Allen, M. T., and Gatto, J. L., *J. Prop. Power* 11:683–697 (1995).
40. Prasad, K., Yetter, R. A., Smooke, M. D., Parr, T. P., and Hanson-Parr, D. M., AIAA paper, 96-0880 AIAA 34th Aerospace Sciences meeting, Reno, January 1996.
41. Tanoff, M. A., Ilincic, N., Smooke, M. D., Yetter, R. A., Parr, T. P., and Hanson-Parr, D. M., *Proc. Combust. Inst.* 27:2397–2404 (1998).
42. Keller, J. O., and Westbrook, C. K., *Proc. Combust. Inst.* 21:547–555 (1986).
43. Keller, J. O., Bramlette, T. T., Dec, J. E., and Westbrook, C. K., *Combust. Flame* 75:33–44 (1989).
44. Barr, P. K., Keller, J. O., Bramlette, T. T., Westbrook, C. K., and Dec, J. E., *Combust. Flame* 82:252–269 (1990).
45. Keller, J. O., Bramlette, Westbrook, C. K., and Dec, J. E., *Combust. Flame* 79:151–161 (1990).
46. Liss, W. E., Thrasher, W. H., Steinmetz, G. F., Chowdiah, P., and Attari, A., *Variability of Natural Gas Composition in Select Major Metropolitan Areas of the United States,* GRI report 92-0123, Gas Research Institute, Chicago, 1992.
47. Held, T. J., and Dryer, F. L., *Proc. Combust. Inst.* 25:901–908 (1994).
48. Koert, D. N., Pitz, W. J., Bozzelli, J. W., and Cernansky, N. P., *Proc. Combust. Inst.* 26:633–640 (1996).
49. Dagaut, P., Reuillon, M., and Cathonnet, M., *Combust. Flame* 101:132–140 (1995).

50. Griffiths, J. F., Halford-Maw, P. A., and Rose, D. J., *Combust. Flame* 95:291–306 (1993).
51. Minetti, R., Carlier, M., Ribaucour, M., Therssen, E., and Sochet, L. R., *Combust. Flame* 102:298–309 (1995).
52. Park, P., and Keck, J. C., SAE paper 90-0027.
53. Ribaucour, M., Minetti, R., Sochet, L. R., Curran, H. J., Pitz, W. J., and Westbrook, C. K., *Proc. Combust. Inst.* 28:xxx–xxx (2000).
54. Cox, A., Griffiths, J., Mohamed, C., Curran, H. J., Pitz, W., and Westbrook, C. K.,*Proc. Combust. Inst.* 26:2685–2692 (1996).
55. Westbrook, C. K., Curran, H. J., Pitz, W. J., Griffiths, J. F., Mohamed, C., and Wo, S. K., *Proc. Combust. Inst.* 27:371–378 (1998).
56. Pollard, R. T., in *Comprehensive Chemical Kinetics, vol. 17*, (C. H. Bamford and C. F. H. Tipper, eds.) Elsevier, New York, 1977, pp. 249–367.
57. Westbrook, C. K., Creighton, J., Lund, C. M., and Dryer, F. L., *J. Phys. Chem.* 81:2542–2554 (1977).
58. Westbrook, C. K., Pitz, W. J., and Leppard, W. R., SAE paper 91-2314.
59. Baldwin, R. R., Pickering, I. A., and Walker, R. W., *J. Chem. Soc. Faraday Trans.* 76:2374–2382 (1980).
60. McAdam, K. G., and Walker, R. W., *J. Chem. Soc. Faraday Trans. 2* 83:1509–1517 (1987).
61. Wagner, A. F., Slagle, I. R., Sarzynski, D., and Gutman, D., *J. Phys. Chem.* 94:1853–1868 (1990).
62. Bozzelli, J. W., and Dean, A. M., *J. Phys. Chem.* 94:3313–3317 (1990); Venkatesh, P. K., Dean, A. M., Cohen, M. H., and Carr, R. W., *J. Chem. Phys.* 111:8313–8329 (1999).
63. Miller, J. A., Klippenstein, S. J., and Robertson, S. H., *Proc. Combust. Inst.* 28:1479–1486 (2000).
64. Bozzelli, J. W., and Pitz, W. J., *Proc. Combust. Inst.* 25:783–791 (1994).
65. Koert, D. N., Pitz, W. J., Bozzelli, J. W., and Cernansky, N. P., *Proc. Combust. Inst.* 26:633–640 (1996).
66. Curran, H. J., Gaffuri, P., Pitz, W. J., Westbrook, C. K., and Leppard, W. R., *Proc. Combust. Inst.* 26:2669–2677 (1996).
67. Curran, H. J., Gaffuri, P., Pitz, W. J., and Westbrook, C. K., *Combust. Flame* 114:149–177 (1998).
68. Benson, S. W., *Proc. Combust. Inst.* 21:703–711 (1986).
69. Benson, S. W., *J. Am. Chem. Soc.* 87:972 (1965).
70. Halstead, M. P., Kirsch, L. J., Prothero, A., and Quinn, C. P., *Proc. Roy. Soc. A* 346:515 (1975).
71. Morley, C., *Proc. Combust. Inst.* 22:911–918 (1988).
72. Cox, R. A., and Cole, J. A., *Combust. Flame* 60:109 (1985).
73. Hu, H., and Keck, J., SAE paper 87-2110.
74. Cowart, J. S., Keck, J. C., Heywood, J. B., Westbrook, C. K., and Pitz, W. J., *Proc. Combust. Inst.* 23:1055–1062 (1990).
75. Smith, J. R., Green, R. M., Westbrook, C. K., and Pitz, W. J., *Proc. Combust. Inst.* 20:91–100 (1985).
76. Cernansky, N. P., Green, R. M., Pitz, W. J., and Westbrook, C. K., *Combust. Sci. Technol.* 50:3–25 (1986).
77. Westbrook, C. K., Warnatz, J., and Pitz, W. J., *Proc. Combust. Inst.* 22:893–901 (1988).
78. Chevalier, C., Pitz, W. J., Warnatz, J., Westbrook, C. K., and Melenk, H., *Proc. Combust. Inst.* 24:93–101 (1992).
79. Leppard, W. R., unpublished data, 1995.
80. Blin-Simiand, N., Rigny, R., Viossat, V., Circan, S., and Sahetchian, K., *Combust. Sci. Technol.* 88:329–348 (1993).
81. Benson, S. W., *J. Phys. Chem.* 92:1531–1533 (1988).
82. Pitz, W. J., and Westbrook, C. K., *Combust. Flame* 63:113–133 (1986).
83. Dec, J. E., SAE paper 97-0873.
84. Flynn, P. F., Durrett, R. P., Hunter, G. L., zur Loye, A. O., Akinyemi, O. C., Dec, J. E., and Westbrook, C. K., SAE paper 1999-01-0509.
85. Stein, Y., Yetter, R. A., Dryer, F. L., and Aradi, A., SAE paper 1999-01-1504.
86. Frenklach, M., and Wang, H., *Proc. Combust. Inst.* 23:1559–1566 (1990).
87. Marinov, N. M., Pitz, W. J., Westbrook, C. K., Vincitore, A. M., Castaldi, M. J., Senkan, S. M., and Melius, C. F., *Combust. Flame* 114:192–213 (1998).
88. Harris, S. J., Weiner, A. M., Blint, R. J., and Goldsmith, J. E. M., *Proc. Combust. Inst.* 21:1033–1045 (1986).
89. Miller, J. A., and Melius, C. F., *Combust. Flame* 91:21–39 (1992).
90. Miyamoto, N., Ogawa, H., Nurun, N. M., Obata, K., Arima, T., SAE paper 98-0506.
91. Onishi, S., Jo, S. H., Shoda, K., Jo, P. D., and Kato, S., SAE paper 79-0501.
92. Noguchi, M., Tanaka, Y., Tanaka, T., and Takeuchi, Y., SAE paper 79-0840.
93. Najt, P. M., and Foster, D. E., SAE paper 83-0264.
94. Akagawa, H., Miyamoto, T., Harada, A., Sasaki, S., Shimazaki, N., Hashizuma, T., and Tsujimura, K., SAE paper 1999-01-0183.
95. Yokota, H., Kudo, Y., Nakajima, H., Kakegawa, T., and Suzuki, T., SAE paper 97-0891.
96. Ishii, H., Koike, N., Suzuki, H., and Odaka, M., SAE paper 97-0315.
97. Hashizume, T., Miyamoto, T., Akagawa, H., and Tsujimura, K., SAE paper 98-0505.
98. Aceves, S. M., Smith, J. R., Westbrook, C. K., and Pitz, W. J., *ASME J. Eng. Gas Turb. Power* 121:569–574 (1999).
99. Aceves, S. M., Flowers, D. L., Westbrook, C. K., Smith, J. R., Pitz, W. J., Dibble, R., Christensen, M., and Johansson, B., SAE paper 2000-01-0327.
100. Kelly-Zion, P. L., and Dec, J. E., *Proc. Combust. Inst.* 28:1187–1194 (2000).
101. Christensen, M., Johansson, B., Amneus, P., and Mauss, F., SAE paper 98-0787.
102. Christensen, M., Johansson, B., and Einewall, P., SAE paper 97-2874.
103. Flynn, P. F., Hunter, G. L., Farrell, L. A., Durrett, R. P., Akinyemi, O. C., zur Loye, A. O., Westbrook, C. K., and Pitz, W. J., *Proc. Combust. Inst.* 28:1211–1218 (2000).

COMMENTS

Christian Eigenbrod, ZARM, University of Bremen, Germany. You were talking nicely, and pretty imaginatively, about staged ignition in diesel engines. But, as with putting a droplet of water into wine, in diesel engines the physical processes of vaporization and mixing are not completely over when autoignition happens; the process must be taken into account. As remaining droplets pin the temperature in their vicinity close to their boiling temperature, the gradient field affects the chemical process leading to autoignition in a much more complex way than homogeneous gas-phase shock tube conditions can unveil.

Author's Reply. The limited time available for my oral presentation resulted in my inability to describe the diesel ignition problem in the detail it deserves. As noted by Dr. Eigenbrod, vaporization and mixing make this a very complex problem. The overall problem and our kinetic modeling of it are described in considerable detail by Flynn et al., based on the experimental laser diagnostics work of John Dec from Sandia National Laboratories. That modeling analysis reinforces the point being made in the lecture that the key chain-branching reaction path in diesel ignition is the same intermediate temperature path that controls engine knock ignition, homogeneous charge compression ignition (HCCI), and rapid compression machine ignition, the decomposition of hydrogen peroxide.

A full model of diesel ignition would certainly have to include fluid mechanics, liquid fuel vaporization, and spatial transport of heat and chemical species. This type of model is being attempted at the present time by a number of researchers. The point of the present work is that simplified kinetic models, making a number of assumptions, are able to establish the major reaction paths that lead to ignition. Quantitative, predictive models will require more detail in their description of these physical processes.

One major point of the paper is that shock tube ignition is the idealized form of high-temperature ignition, while diesel ignition is an applied example of intermediate-temperature ignition. Therefore, the two processes are controlled by different kinetic reaction mechanisms.

•

Arvind Atreya, University of Michigan, USA.

1. From your excellent lecture, it appears that ignition and extinction are two sides of the same coin. I agree. Could you comment on this?
2. If the above is true, there seems to be a discrepancy in temperatures at ignition and extinction. Experiments by Tsuji and coworkers show that the temperature at extinction for hydrocarbon flames is about 1450 K, whereas your ignition temperatures are around 1100 K. Is it possible that extinction follows the high T branch?

Author's Reply. In another paper at this same symposium [1], we used kinetic modeling to reproduce the work of Tsuji et al. cited by Prof. Atreya, which was also reported by Law and Egolfopoulos. The works of Tsuji et al. and Law et al. deal with extinction of atmospheric pressure hydrocarbon flames at temperatures of about 1450 K. We extended these calculations to engine pressures of 50–100 bar to show that the extinction temperature increases to about 1900 K, with profound implications about emissions of NO_x. Our modeling work attributes this extinction to suppression of the high-temperature chain-branching reaction pathway, as Prof. Atreya indicates. The ignition temperatures of 1100 K cited in his question describe different problems including engine knock and early premixed ignition in diesel engines, not flame propagation. Therefore, I disagree with his proposition that ignition and extinction are parts of the same problem.

REFERENCE

1. Flynn, P. F., Hunter, G. L., Farrell, L. A., Durrett, R. P., Akinyemi, O. C., Westbrook, C. K., and Pitz, W. J., *Proc. Combust. Inst.* 28:1211–1218 (2000).

•

Norbert Peters, RWTH Aachen, Germany. In the intermediate temperature range of *n*-heptane ignition, radical runaway at the second ignition is triggered by the depletion of the fuel which is the chain-breaking agent during the period after the first-stage ignition. Hydrogen peroxide decomposition provides the radicals needed for fuel consumption, but its temperature dependence is not a determining factor because the temperature is nearly constant during this period. If it was, hydrogen peroxide would decrease rather then increase during this period.

•

Russell Lockett, City University, UK. A dynamical systems analysis of methanol autoignition reveals that thermal runaway begins at the maximum of the hydrogen peroxide concentration profile. This maximum also defines a bifurcation in the system. Therefore, autoignition is defined by the decomposition of hydrogen peroxide. I would expect this to be true of the thermal runaway in two-stage ignition as well.

Author's Reply. In answer to the previous two comments, it is tempting to try to simplify these kinetic systems to make them easy to understand. A linear model is frequently most satisfying: A leads to B leads to C. In these kinetic problems, several processes happen together to

cause the thermal runaway of ignition, and it is not clear that any of them can be identified as the "cause." It is most useful to recall the different processes that occur and the conditions required for each of them. Hydrogen peroxide requires a temperature of 1000–1100 K to decompose, and its decomposition provides lots of OH radicals. Hydrocarbon fuels react rapidly with radical species such as OH, O, and H. Rates of reaction with these radicals are much greater with hydrocarbons than with species such as CO and H_2, which produce rapid heat release. The presence of hydrocarbon effectively inhibits these heat releasing reactions, so hydrocarbons inhibit ignition.

•

John Griffiths, University of Leeds, UK. I recognize the need for economy of discussion in a wide-ranging review, but I am concerned by the simplification that there is a "critical decomposition temperature" for the H_2O_2 intermediate. This is open to misinterpretation because the event is not a "criticality" but a subtle interaction between the amount of H_2O_2 formed and the evolving temperature of the reactants. As you have noted, the influence of temperature is dominant because the activation energy for decomposition is so high. The chain-thermal feedback as the decomposition proceeds leads to an acceleration that may look like a "critical condition" for temperature (and even concentration, maybe), but it is not so. There are relationships also to the duration of events in the lead up to the "proper ignition" through the "starting" temperature and the rate at which H_2O_2 is generated. The higher the "ceiling temperature" for the $R + O_2/RO_2$ equilibrium, the shorter will be that second stage: the system is given a reduced handicap (which is governed by the RO_2 structure)! The H_2O_2 formation obviously relies on HO_2, but I am inclined to single out CH_2O as an important molecular intermediate in this stage because all routes for its oxidation lead to HO_2. The relevance of CH_2O in the development of the second stage was discussed by Gibson et al. [1].

REFERENCE

1. Gibson, C., Gray, P., Griffiths, J. F., and Hasko, S. M., *Proc. Comb. Inst.* 20:101–109 (1984).

Author's Reply. The analysis included in the present paper on critical temperatures for decomposition of H_2O_2 was taken directly from the work of Prof. Griffith. He and I have communicated many times on these issues. This comment is another example of the fact that kinetic systems are extremely complex, even when all the rate constants are known. Professor Griffith and his collaborators have studied the mathematical issues associated with ignition, providing important insights about critical phenomena. The identification of the ceiling temperature as an important metric for this type of problem has been discussed at length, and it is clearly important. The idea of the importance of formaldehyde as a major molecular intermediate is interesting but not yet supported by any kinetic evidence. This would be a suitable topic for future research.